GeoExpert ag

swiss*nuclear*: PEGASOS Refinement Project:
SP2 – Ground Motion Characterization

Contract no. PMT-VT-1032

Seismic Shear Wave Velocity Determination and Hybrid Seismic Survey at the SED-Station LLS (Linth-Limmern GL)

Date of Field Data Acquisition 30th March 2009

Report

Client

swiss*nuclear*
Project PRP
Frohburgstrasse 17
4601 Olten

Contractor

GeoExpert ag
Seismic Prospecting
Ifangstrasse 12b
P.O. Box 451
8603 Schwerzenbach

8603 Schwerzenbach, 29th May 2009

INDEX

1 INTRODUCTION

1.1 Survey objectives

The seismic survey's main task is to provide information about the distribution function of the shear wave velocities in the depth interval of the uppermost 30 m along a 100 m long seismic profile.

Additionally, the following objectives are to be met:

- the mapping of the topography of the rock face, i.e. the thickness of the Quaternary deposits;
- the determination of the thickness of the weathered zone and its degree of decompaction at the bedrock surface;
- a general view of geological structures.

1.2 The choice of the appropriate surveying methods

Several methods are available for deriving the s-wave velocity distribution in the subsurface at any given position:

- in-situ measurement by down-hole or crosshole seismic surveying;
- shear-wave refraction tomography profiling;
- dispersion analysis of surface waves (MASW; **M**ultiple channel **A**nalysis of **S**urface **W**aves)

The surveys are to be carried out at, or as close as possible near some 20 SED earth quake monitoring stations in Switzerland. Ideally, the surveys are to be conducted on two orthogonal profiles in order to derive at their point of intersection a robust 1D s-wave velocity distribution function by correlation. To this end, the methods of MASW and shear-wave refraction tomography profiling are to be combined.

The results are to include the following fundamental parameters $v_{s,5}$, $v_{s,10}$, $v_{s,20}$, $v_{s,30}$, $v_{s,40}$, $v_{s,50}$, $v_{s,100}$ are to be calculated, also an error estimation of all values.

The data acquired for the MASW method are to be subjected to complementary **p-wave hybrid seismic data processing** in order to image the geological structures.

2 FIELD DATA ACQUISITION PARTICULARS

2.1 Time Schedule

Date	*Time*	*Activities / remarks*
30.03.2009	0730	arrival from Schwerzenbach
	0730 - 0845	dislocation to the cavern
	0845 - 0900	site reconnaissance
	0900 - 1015	lay-out of recording spread profile 1 p- and s-wave
	1015 - 1030	tests
	1030 - 1115	compressional wave data recording profile 1
	1130 - 1155	shear wave data recording profile 1
	1155 - 1230	retrieval of the recording spread
	1330	departure from cavern
	1420	departure from site

2.2 Summary of Data Acquisition Parameters

Compressional Wave Data Acquisition

# of active channels	96
geophone type	4.5 Hz natural frequency, vertical velocimeter
receiver station spacing	1.5 m
# of geophones/station	1
source point spacing	3.0 m
source type	vertical hammer (6 kg) striking on the concrete foundation
sampling rate	500 µs
recording time	2048 ms
field filters	0.5 Hz LC, anti-alias
# of field records	70

Shear Wave Data Acquisition

# of active channels	48
geophone type	10 Hz natural frequency, horizontal velocimeter
receiver station spacing	3.0 m
# of geophones/station	1
source point spacing	6.0 m
source type	horizontal hammer (6 kg) striking horizontally at the gallery's socket
sampling rate	500 µs
recording time	512 ms
field filters	2 Hz LC, anti-alias
# of field records	50 at 25 positions

Fig. 2.1: Seismic data acquisition in the gallery. The yellow boxes contain 24 A/D-converters each. In the background the seismic observation station.

2.3 Composition of Seismic Field Crew

Personnel

Lorenz Keller	dipl. Natw. ETHZ, geophysicist, party chief
Jochen Fiseli	Dipl.-Geologe, University of Freiburg I. Br.
Kieron Lynch	assistant, spread lay-out and activation of seismic source

Equipment

96	vertical geophones 4.5 Hz
48	horizontal geophones 12 Hz
6	seismic cables
1	seismic acquisition system Summit Compact, 96 channels
1	laptop computer for data acquisition
3	walkie-talkies
1	hammer 6 kg
1	steel plate
1	metal-plated wooden beam
1	van (FIAT Ducato 4x4)

2.4 Location

The seismic monitoring station LLS (Linth-Limmern dam, Linthal GL) is situated in a gallery in hard layered limestone sediments near Linth-Limmern dam. Some 500 m away, a geological window opens into Triassic sediments and the crystalline basement

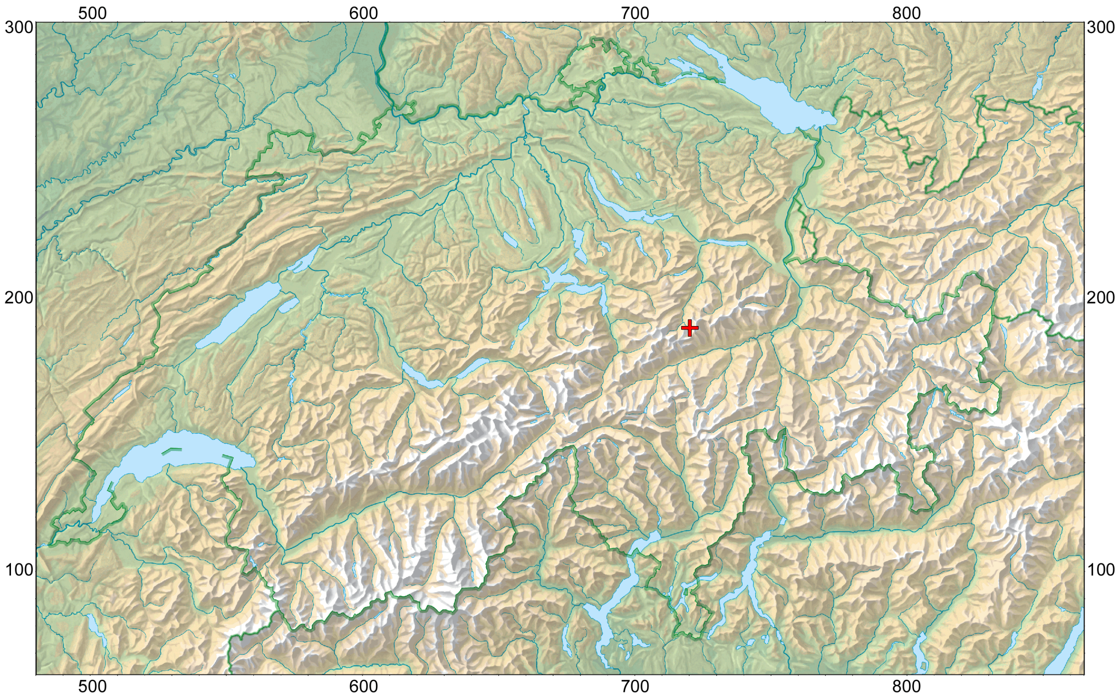

Fig. 2.2: The red cross marked seismic monitoring station LLS (Linth-Limmern dam, Linthal GL) is located in Glarus' mesozoic sediments (Malm). (map: geodata @ swisstopo).

2.5 Recording Conditions and Line Setup

The seismic data acquisition was done in the galleries of Linth-Limmern dam corporation. The seismic observation station lies in a small cavern directly besides the "Fensterstollen" in which the 150 m array of geophones was placed. The gallery has a concrete basement of about 50 cm, in which small holes were drilled and the geophones are plugged-in.

2.6 Seismic wave generation

The vertical hammer impacts strike at this concrete basement. So in the seismic p-wave records should image a two-layer-case. Each p-wave source lies between two geophones, directly on the geophone layout.

Shear wave data acquisition was expected to be hard to be accomplished. Due to limited space, the shear wave stimulation with the wooden beam utilized at other sites was not possible. Alternatively, hammer strikes on the gallery's walls were done (directly at the nearly unweathered limestone). Because of that, the shear wave sources were usually placed 1.5 m away from the seismic line on both sides of the geophone layout.

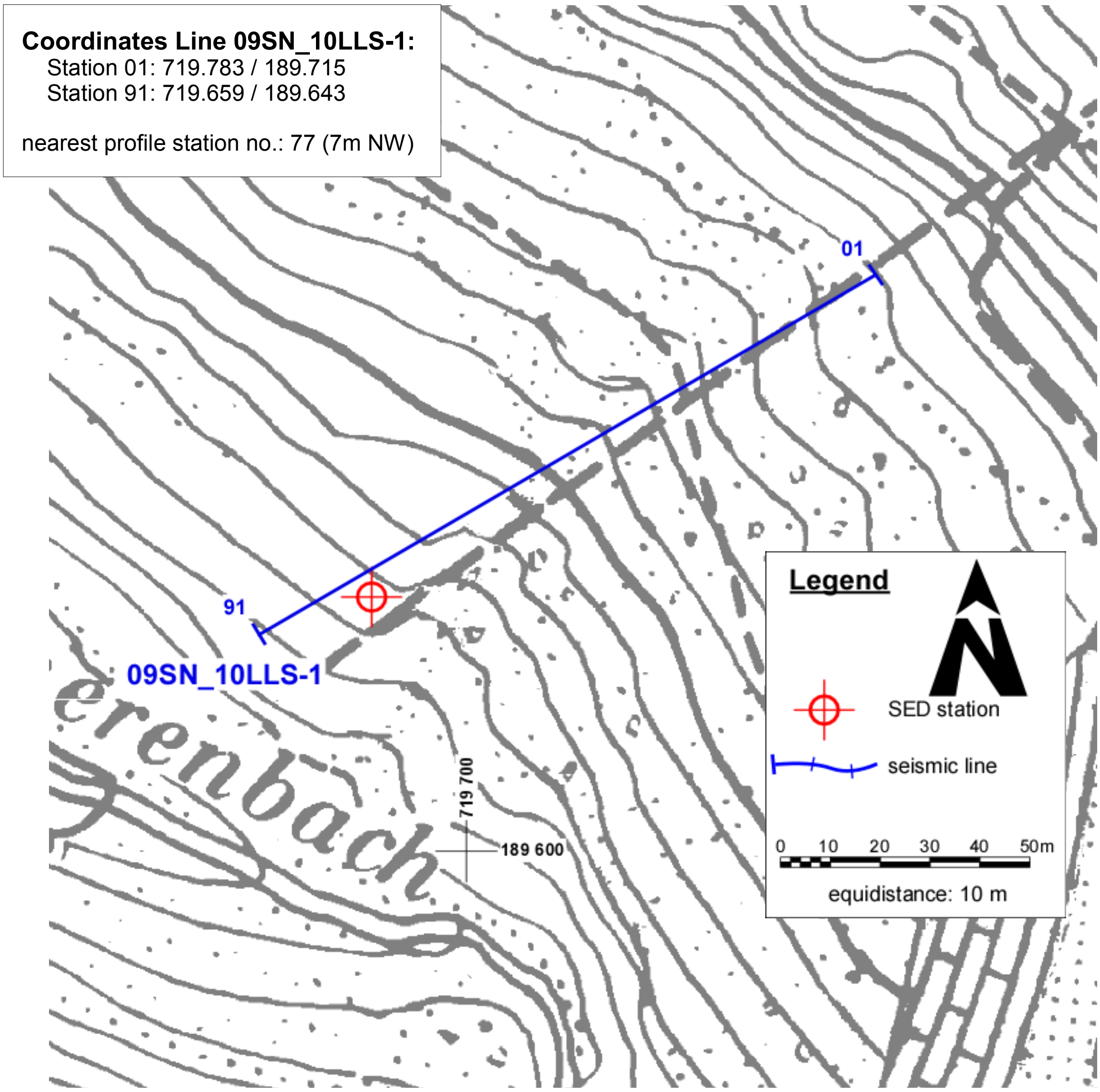

Fig. 2.3: Situation map with the trace of seismic profile 09SN_10LLS-1 (Linth-Limmern dam, GL). (background map: © Kt. Glarus/SWISSFOTO+PK25 © 2008 SWISSTOPO (DV012728.1, DV012446).)

3 SEISMIC DATA PROCESSING AND IMAGING OF THE RESULTS

3.1 General Remarks

- For the shear and compressional wave refraction seismic evaluation the package **RAYFRACT** by Intelligent Resources Ltd., Vancouver CAN, was used. The system features the technique of diving wave tomography (www.rayfract.com).
- The system **SPW** (**S**eismic **P**rocessing **W**orkshop) of Parallel Geoscience Corporation, Austin US-TX, was used for reflection seismic data processing (www.parallelgeo.com).
- Data processing of surface waves (MASW processing) was conducted with the software package **SurfSeis** V2.0 of Kansas Geological Survey in Lawrence US-KS.

A detailed description of the various surveying methods will be included in the general summary report.

3.2 Shear Wave Refraction Tomography

3.2.1 Reformatting and field geometry assignment

After reformatting the field data into the Rayfract format the field geometry is applied.

3.2.2 First break time picking

At each shot position, two seismic records were acquired in both activation directions. These two records are displayed superimposed with different colors on each other in Fig 3.2a together with the manually determined first arrival time picks.

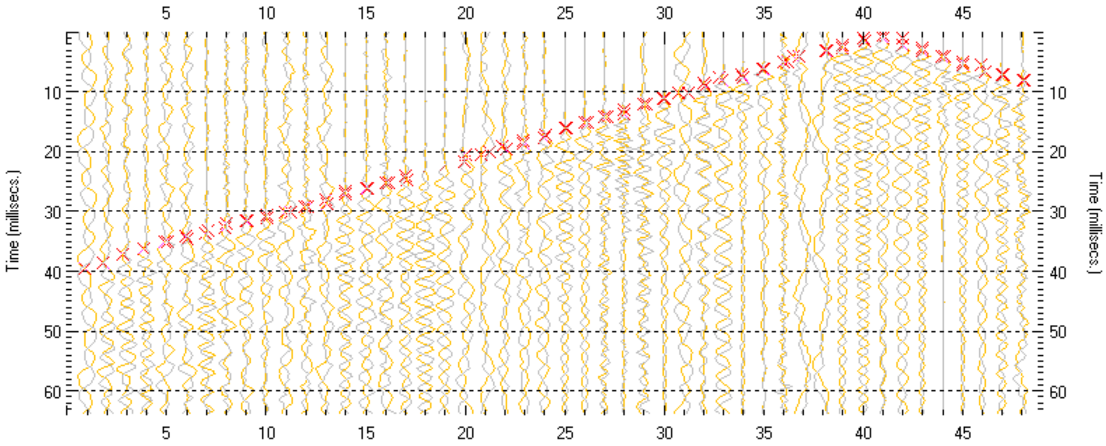

*Fig. 3.2a: High quality dual field record of line 09SN_10LLS-S showing at each station the s-wave traces with opposing polarities in different colors. The manually picked s-wave refraction arrivals at each station are marked with an **x**. The station spacing is 3 m, profile station number 00 = line station number 0; profile station number 45 = line station number 91.*

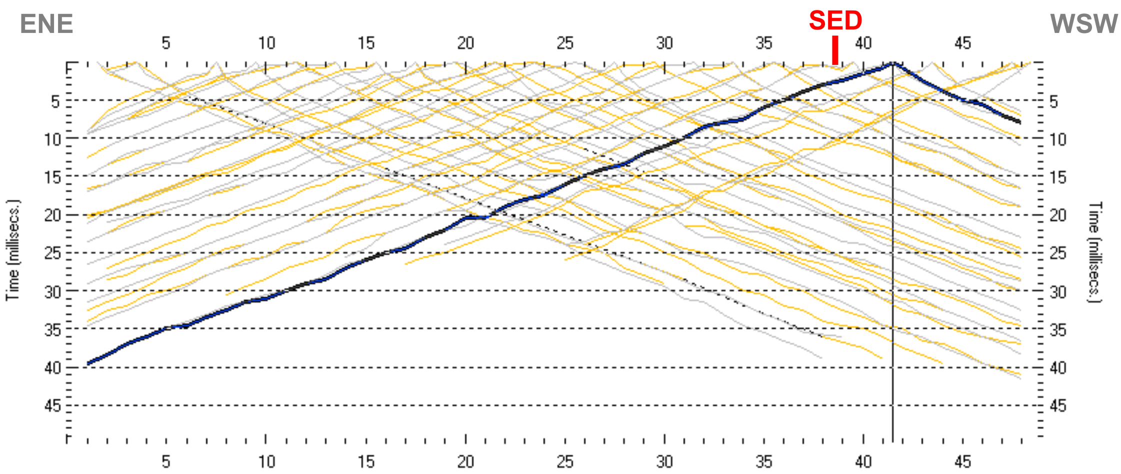

Fig. 3.2b: Curves of s-wave first break time picks of line 09SN_10LLS-S.

3.2.3 Analytical Determination of Refraction Velocities

An initial 1D-velocity function (averaged 1D velocity-depth profiles derived by the Delta-t-V method, see Tab. 3.2a) is determined in the 3-dimensional time-offset-CMP-domain of all first break arrival time curves in the 3-dimensional time-offset-CMP-domain (see. Fig. 3.2c).

Depth [m]	Vs [m/s]
0.0	2256
0.3	2407
0.6	2616
1.0	2680
1.3	2776
1.9	2879
2.5	2927
3.5	2968
4.8	3006
6.2	3051
8.3	3042
11.0	3054
14.3	3187
18.8	3429
24.5	3687
32.1	4286

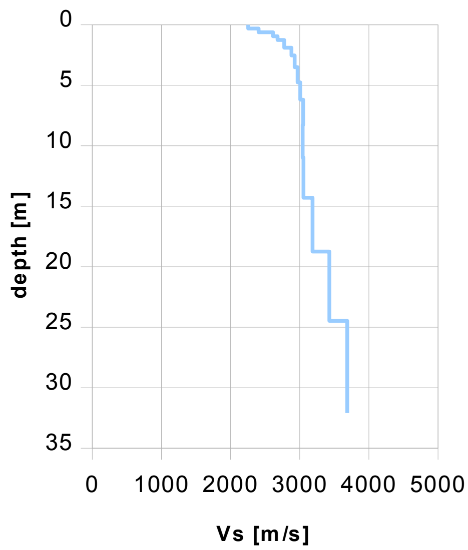

Tab. 3.2a: Initial 1D s-wave velocity function derived from real data of line 09SN_10LLS-S (mean values between line station 30 and 60 (= profile stations 45 - 90)).

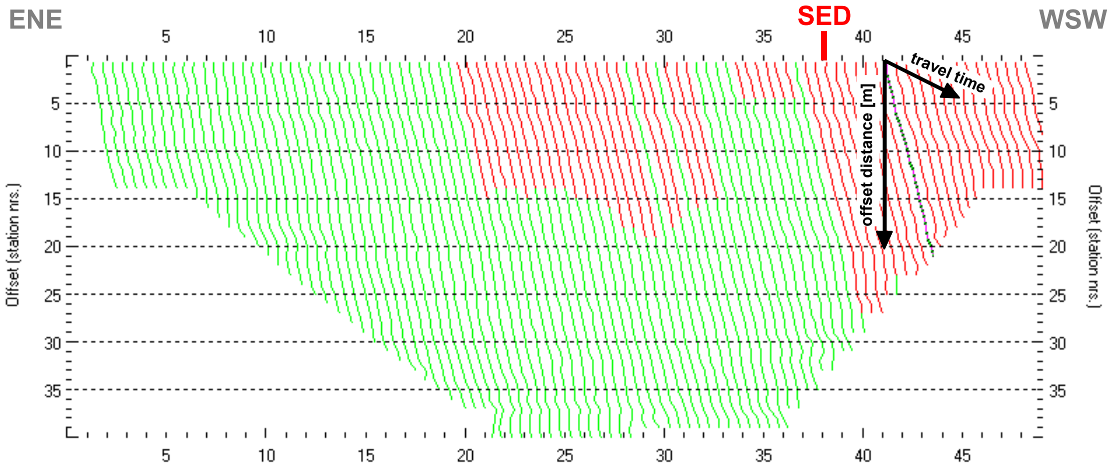

Fig. 3.2c: 3-dimensional distance-travel time diagrams of line 09SN_10LLS-S at the mid-points between source points and receiver stations are instrumental when using the analytical CMP derivation of the initial velocity field.
The horizontal axes are the along the CMP positions and the travel time respectively, the vertical axis denotes the offset distance between source and receiver positions. The colors represent different velocity layers. The station spacing is 3 m, profile station number 0 = line station number 00; profile station number 45 = line station number 91. The colors represent different velocity layers.

3.2.4 Tomographic inversion of the velocity gradient field by iterative modeling

The velocity field is iteratively refined by the subsequent Wavepath Eikonal Traveltime (WET) tomographic inversion process. The inversion results are portrayed in Fig. 3.2d as a gridded velocity contour section and in Fig. 3.2e as a ray path density section.

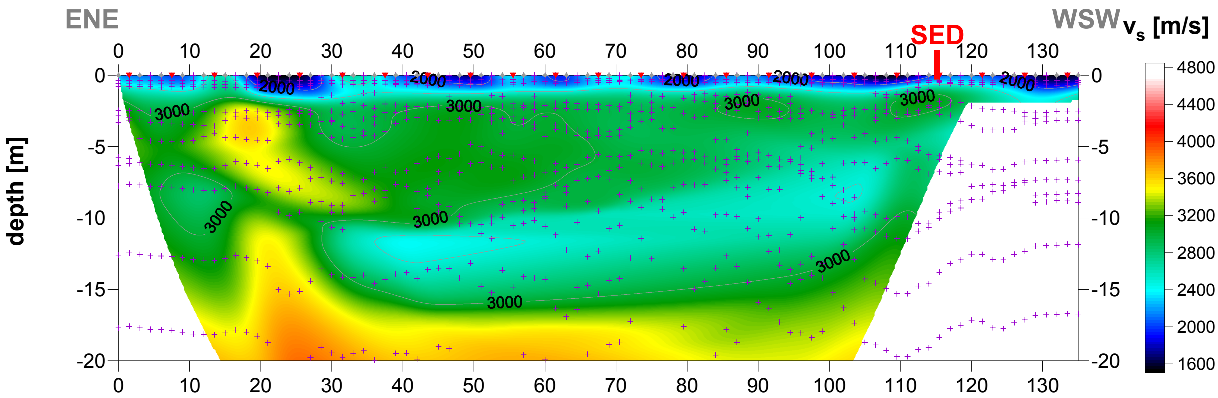

Fig. 3.2d: Shear wave velocity field of line 09SN_10LLS-S. Red/white colors denote solid rock, blue/black colors point to unconsolidated sediments and soil.
Vertical axis: elevation [m a.s.l]; horizontal axis: profile meter; color encoded scale: v_s [m/s]; vertical exaggeration: 2:1; gray diamonds: receiver positions; red triangles: source positions; magenta crosses: positions of determined velocity values. The station spacing is 3 m, profile meter 0 = line station number 00; profile meter 135= line station number 91.

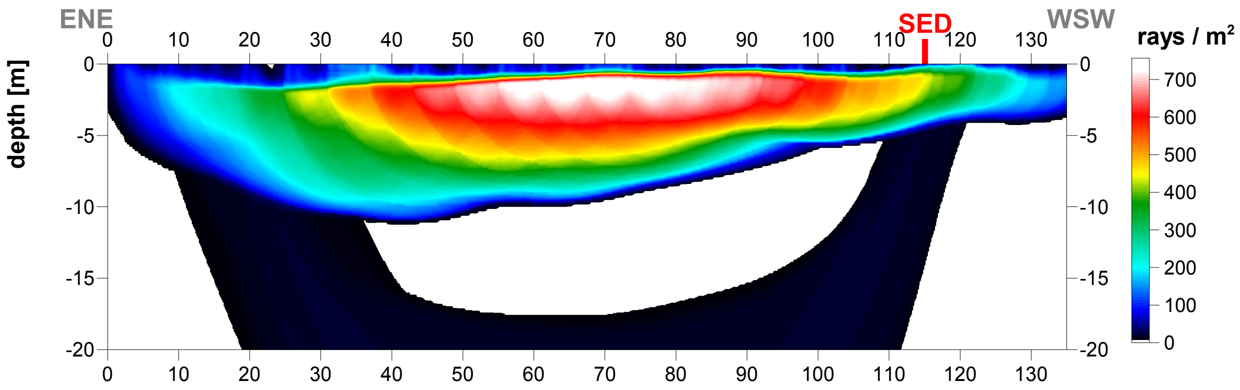

Fig. 3.2e: Shear wave ray path density (coverage) along the seismic line 09SN_10LLS-S. Red/white colors indicate high velocity contrasts (usually at the bedrock surface), blue/black colors denote low coverage areas. Vertical axis: depth [m]; horizontal axis: profile meter; color encoded scale: ray paths per m^2; vertical exaggeration: 2:1. The station spacing is 3 m, profile meter 0 = line station number 00; profile meter 135= line station number 90.

Depth [m]	Vs [m/s]
0.0	2074
2.2	2982
4.4	2978
6.7	2991
8.9	2804
11.1	2570
13.3	2735
15.6	3041
17.8	3468
19.9	3606
22.1	3675
24.3	3779
26.5	3919
28.8	4083
31.0	4253

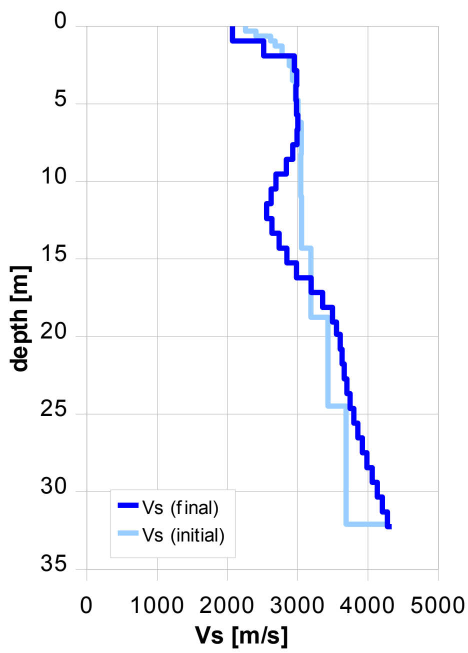

Tab. 3.2b: Final 1D s-wave velocity model derived from real data of line 09SN_10LLS-S (horizontal average of all values) for the profile segment (between line stations 30 and 60) with a geological setting resembling the one at the SED station. The calculated values of the initial 1D s-wave velocity model are given in Tab. 3.2a.

The derived low velocity zone in 12 m depth seems to be artificial due to a velocity gradient near by 0. The velocities below this depth result only by inversion of low coverage data (dark colors in Fig. 3.2e) – they are not reliable.

3.3 MASW Processing

3.3.1 Reformatting and field geometry assignment

The data preparation steps for the dispersion analysis include

- the assignment of the field acquisition geometry
- the selection of suitable offset ranges (=arrays) between 10 m and 50 m for dispersion, and the splitting of the field records in forward and reverse shooting direction data sets
- the reformatting of the data into the specific KGS format

X - - ... - - o-o-o-...-o-o-o (forward shooting or so-called PLUS direction)
respectively
o-o-o-...-o-o-o - - ... - - X (reverse shooting or so-called MINUS direction).

where **X** = shot position
o = receiver station
- = 1.5 m offset

The active array used at SED-station LLS are the receiver station in the shot offset range between 10 and 75 m.

3.3.2 Calculating the dispersion image (overtone)

The result of dispersion analysis is the color encoded acoustic energy distribution in the phase velocity - frequency plane (see Fig. 3.3a and b).

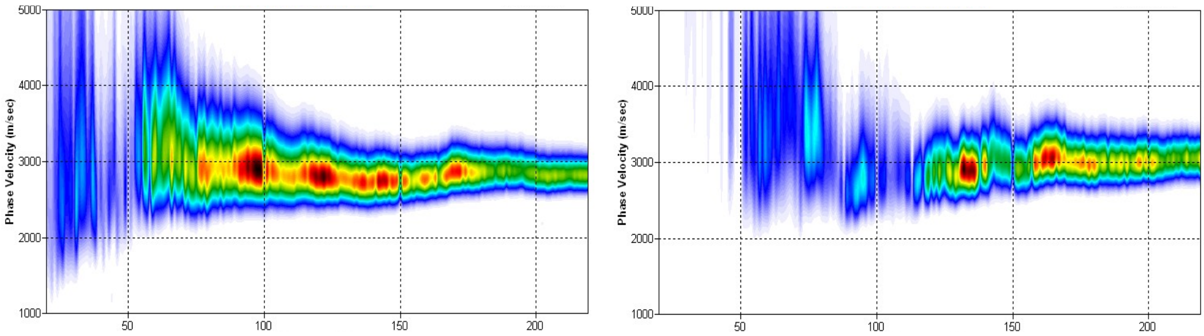

Fig. 3.3a: Dispersion image of high quality data (left) at midpoint station 66 as found on 80 % and of moderat quality data (right) at midpoint station 48 representing about 20 % of the MASW dataset of site LLS.
Horizontal axis: frequency from 20 to 220 Hz; vertical axis: phase velocity from 1000 to 5000 m/s; color code: colors from white (no energy) to blue - green - yellow - red - black point to increasing energy amplitude values.

3.3.3 Analysis of the dispersion image

In the dispersion graphs as calculated in section 3.3.2 above, the curves joining the amplitude peaks of the fundamental modes are determined either by subjective inspection or in a semi-automated manner. On datasets with poorly defined amplitude peaks or with a highly irregular alignment of the peaks, the danger of obtaining improbable or wrong results is real and can only be mitigated by the processing experience and the a-priori knowledge of the geological setting by the geophysicist responsible for the data evaluation.

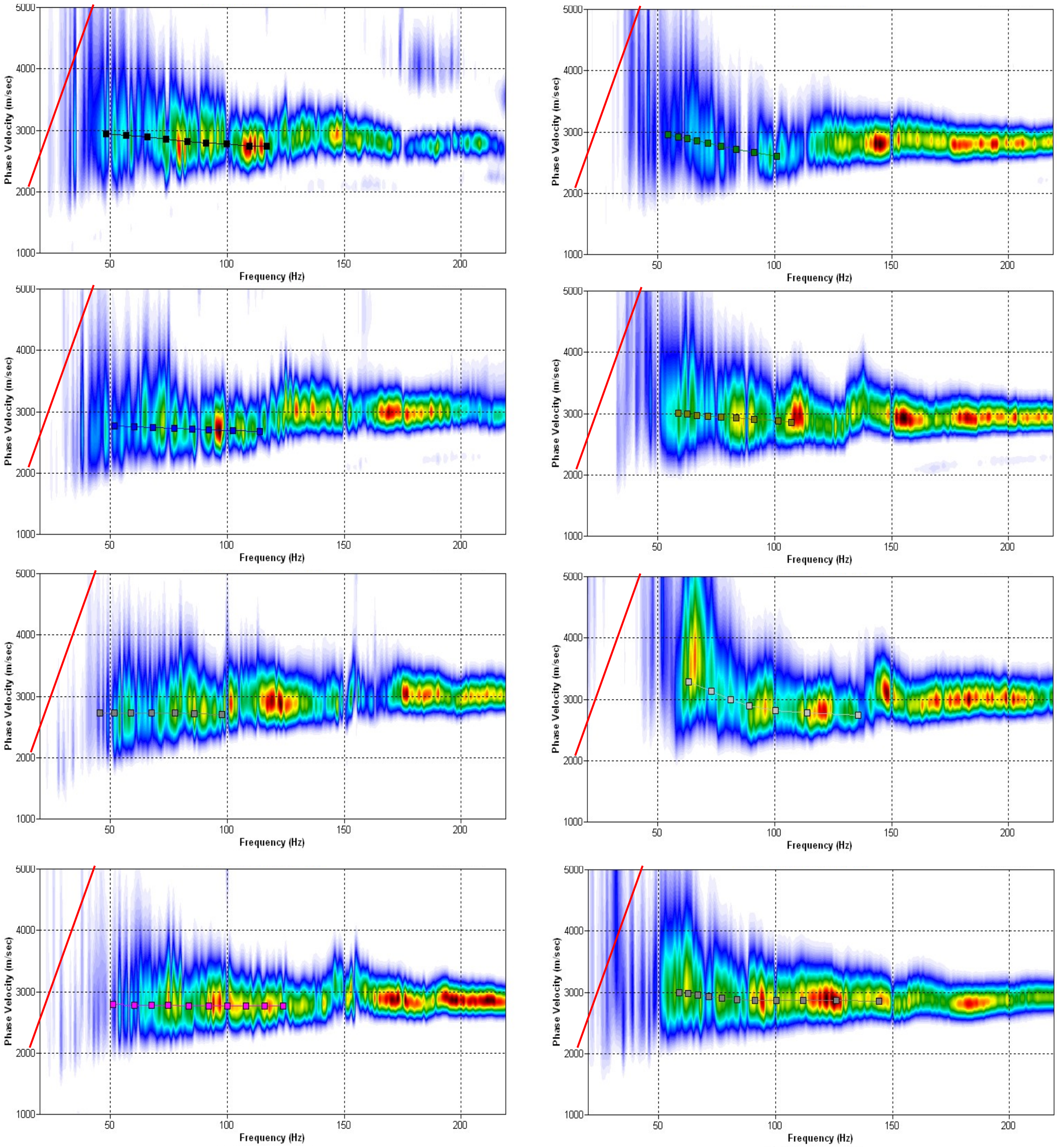

Fig. 3.3b: The manually picked dispersion images used for the derivation of the shear wave velocity section on line 09SN_10LLS-M. The dispersion curves (squares) are determined by linking the peaks of high energy. Note that 'higher modes' may at times produce higher energy peaks than the fundamental mode required for the analysis.
red line: high resolution beam-forming curve for v_{max}.
1st row: left: station 30 @ PLUS direction; right: station 30 @ MINUS direction
2nd row: left: station 40 @ PLUS direction; right: station 40 @ MINUS direction
3rd row: left: station 50 @ PLUS direction; right: station 50 @ MINUS direction
4th row: left: station 62 @ PLUS direction; right: station 60 @ MINUS direction

3.3.4 Inversion of dispersion curves resulting in a 1D shear wave velocity distribution

Inversion of the extracted dispersion curves was performed using the algorithm described by Xia et al. (1999).

The inversion process is started by setting the maximum depth (z_{max}) to be in the order of 30% of the largest wavelength for an initial model consisting of 10 layers of increasing thicknesses. For all 10 layers the Poisson's ratio is assumed to be 0.3 and the rock/soil density to be 2.3 g/cm³. The inversion process is concluded either after twelve iterations or when the convergence condition of a RMS-error of less than 3 m/s (phase velocity) is met.

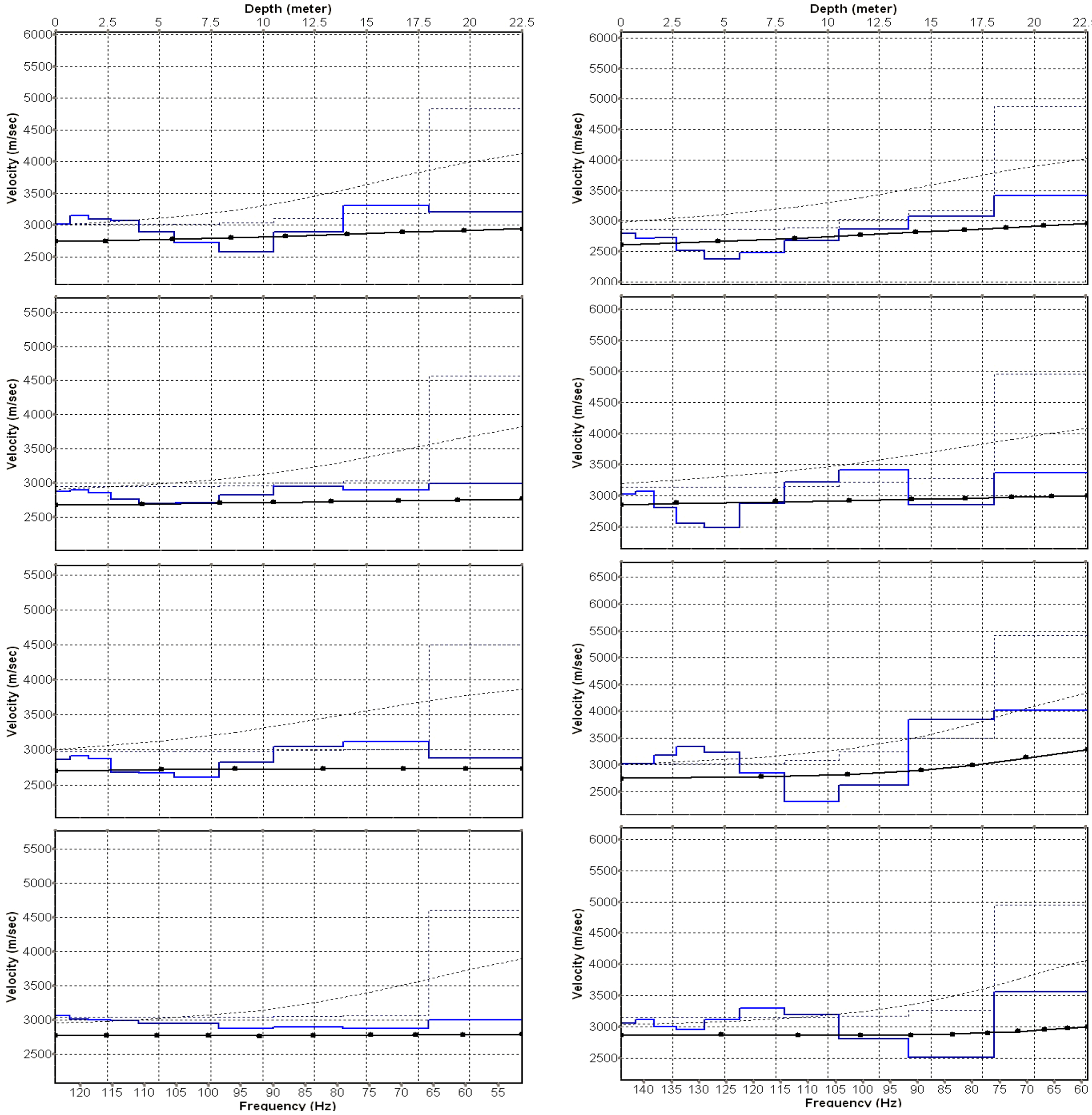

Fig. 3.3c: Inversion results of dispersion curves of dataset at line 09SN_10LLS-M.
***brown**: Inversion of dispersion curve (dots) resp. of the modeled dispersion curve (dotted line: initial model; continuous line: end model). Horizontal axis: frequency Hz, vertical axis: v_s.*
***blue**: 10-layer-model (dotted: initial model, continuous line: final model). Horizontal axis: depth, vertical axis: phase velocity resp. v_s).*
1st row: left: station 30 @ PLUS direction; right: station 30 @ MINUS direction
2nd row: left: station 40 @ PLUS direction; right: station 40 @ MINUS direction
3rd row: left: station 50 @ PLUS direction; right: station 50 @ MINUS direction
4th row: left: station 62 @ PLUS direction; right: station 60 @ MINUS direction

Dispersion analyses of records with longer receiver arrays should – by theory – increase the investigation depth. At LLS, with both directions, MASW processing with the maximal array length of 135 m confirms and improves the results from 65 m arrays (Fig. 3.3d and Fig 3.3f).

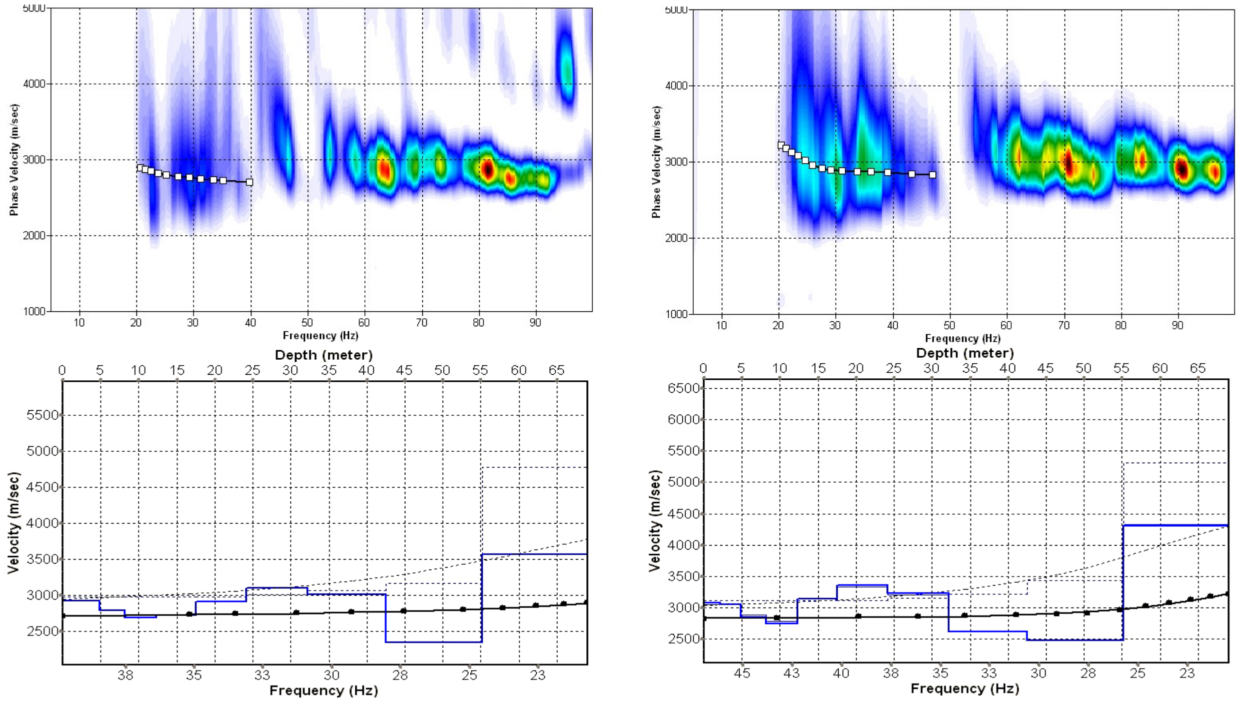

Fig. 3.3d: Top: dispersion images of over-all arrays (30...170 m offset) of line 09SN_10LLS-M in PLUS (left) and of the over-all array (15... 142 m offset) in MINUS (right) direction; dotted fine line: signal-noise ratio for the designated f-v_{ph}-value. Red line: high resolution beam-forming curve for v_{max}.
*Below: The two respective inversion results; **brown**: inversion of dispersion curve; **blue**: 10-layer-model. Horizontal axis: depth, vertical axis: phase velocity resp. v_S.*

3.3.5 Gridding and plotting of 2D v_s-velocity field

By assembling the 1D v_S - depth functions of all stations the final 2D v_S-field is derived using a Kriging gridding procedure as portrayed in Fig. 3.3e below:

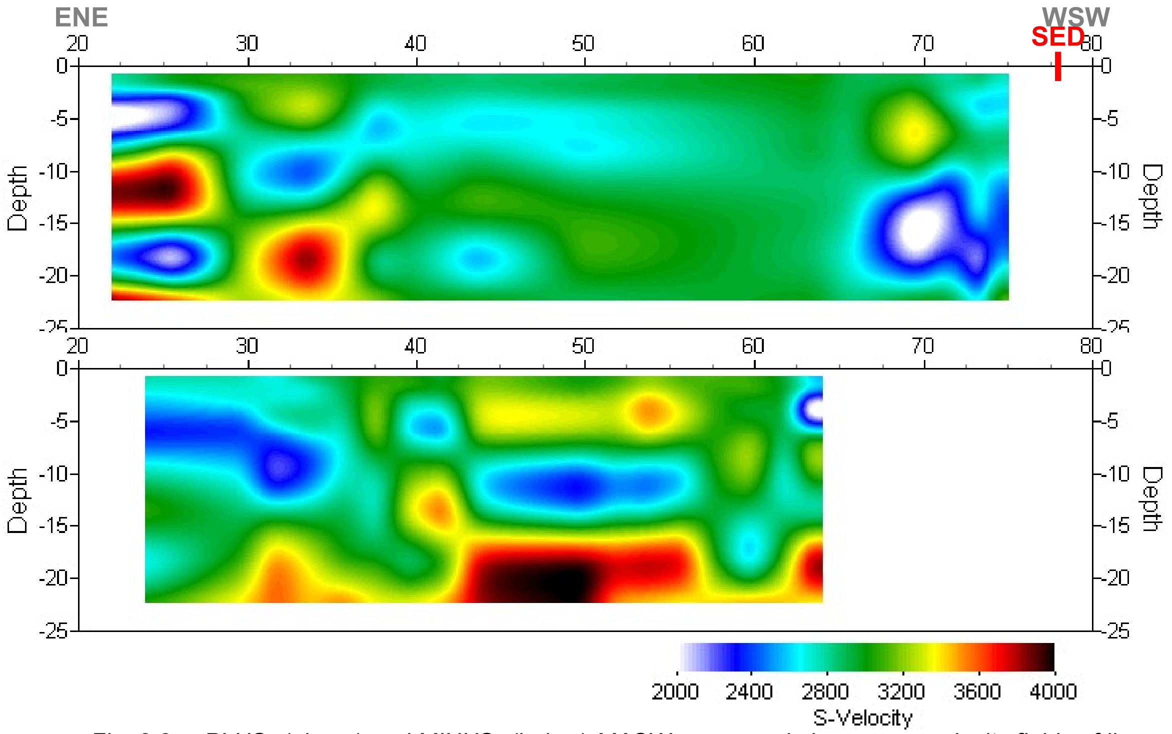

Fig. 3.3e: PLUS- (above) and MINUS- (below)-MASW-processed shear wave velocity fields of line 09SN_10LLS-M. Profile station number 20 = profile meter 30, station spacing is 1.5 m.

3.3.6 Calculation of the average shear wave velocity

In order to calculate a representative shear wave velocity-depth function of line 09SN_10LLS-M at the SED station, all computed 1D-v_S-depth functions between seismic profile station no. 30 and 60 are averaged (non-weighted mean values). The v_S-depth-function is shown in Tab. 3.3a.

Depth [m]	Vs- [m/s]	Vs+ [m/s]	Vs [m/s]
0.7	3015	2920	2968
1.6	3034	2943	2989
2.7	3048	2909	2978
4.0	3066	2789	2928
5.7	2992	2707	2849
7.9	2849	2675	2762
10.5	2721	2851	2786
13.9	2933	3115	3024
18.1	3310	3038	3174
22.6	3530	3096	3313

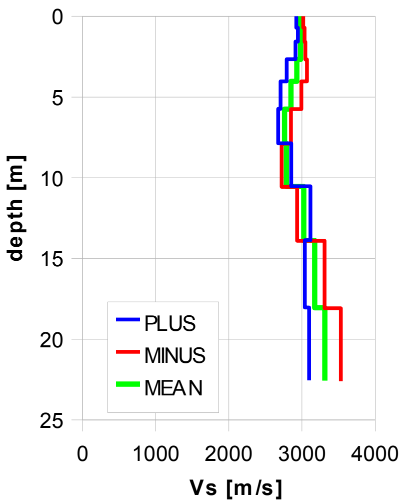

Tab. 3.3a: Averaged vs - depth function of line 09SN_10LLS-M at the SED station. Blue line: MASW-'PLUS' processing, red line: MASW-'MINUS' processing; green line: average of PLUS- and MINUS-functions.

The inversion of the four 135 m-array dispersion curves data (15 to 142 m offset (MINUS) resp. 30 to 170 m (PLUS), see Fig. 3.3D) are given in Tab. 3.3B. These values are complemented with the values derived of the 65 m-array analyses (Tab. 3.3a).

135 m array				65 m array			
depth	**m1+**	**m1-**	**m**	**depth**	**65 -**	**65 +**	**65**
2.1	2917	3083	3000	0.7	3015	2920	2968
4.8	2918	3050	2984	1.6	3034	2943	2989
8.2	2790	2854	2822	2.7	3048	2909	2978
12.3	2684	2743	2713	4.0	3066	2789	2928
17.6	2720	3137	2928	5.7	2992	2707	2849
24.1	2909	3363	3136	7.9	2849	2675	2762
32.3	3100	3238	3169	10.5	2721	2851	2786
42.5	3010	2619	2815	13.9	2933	3115	3024
55.2	2338	2485	2412	18.1	3310	3038	3174
69.0	3562	4312	3937	22.6	3530	3096	3313

Tab. 3.3b: v_S-depth values of the four MASW-derived dispersion curves of both 135 m and 65 m arrays of seismic line 09SN_10LLS-M.

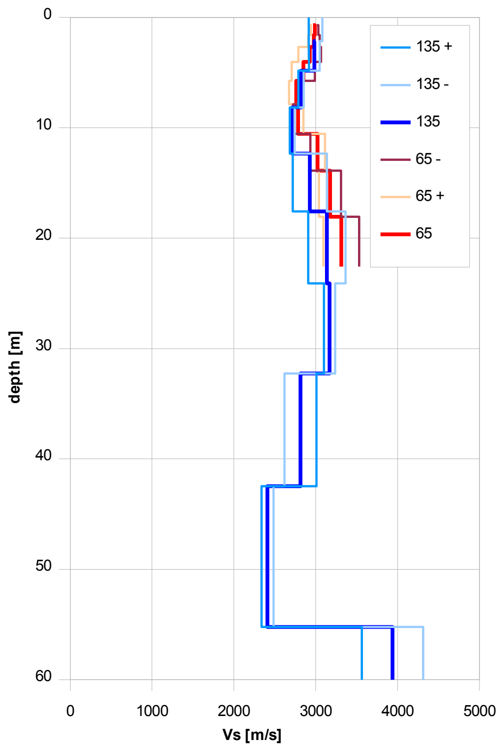

Fig. 3.3f: Comparison of the ensemble of inversion results of line 09SN_10LLS-M, either using the 65 m- and the 135 m-arrays.
blue lines: analyses of 135 m arrays of line 09SN_10LLS-M
red lines: analyses of 65 m arrays of line 09SN_10LLS-M
bold lines: mean of both direction analyses.

3.3.7 Calculation of the shear wave velocity scalars $v_{s,5}$, $v_{s,10}$, ...

The parameters $v_{s,5}$, $v_{s,10}$, $v_{s,15}$, $v_{s,20}$, $v_{s,25}$ represent the average shear wave velocities in the depth interval between the surface and the respective depth levels and are determined by the formula

$$v_{s,n} = \frac{\sum_{i=1}^{n} d_i}{\sum_{i=1}^{n} d_i / v_{si}}$$

with:

d_i = thickness of layer i
v_{si} = corresponding shear-wave velocity.

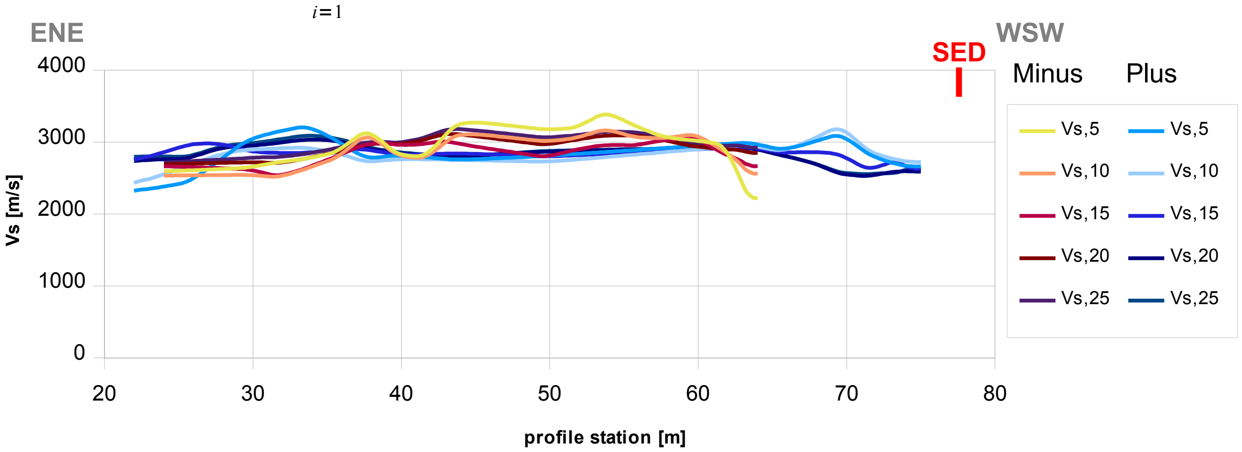

Fig. 3.3g: Graphs of the averaged vs,5...-values along the line 09SN_10LLS-M for the PLUS- (blue lines) and MINUS- (red lines) directions.

The average values of the s-wave velocity model $v_{s,5}$, $v_{s,10}$, $v_{s,15}$, $v_{s,20}$, $v_{s,25}$ (= average shear wave velocity from the surface to depths of 5 m, …until 100 m) on the line segment nearest to the SED station (Tab. 3.3d) are summarized below:

	Vs,5	Vs,10	Vs,15	Vs,20	Vs,25	Vs,30
MINUS	3081	3035	2937	2991	3065	n/a
PLUS	2893	2806	2850	2896	2911	n/a
MEAN	2987	2920	2893	2943	2988	n/a

Tab. 3.3d: The average shear wave velocities within the depth intervals from surface down to 5 m, etc.… to 25 m, calculated for the line segment with a subjectively most similar geology to the SED station (profile station 30 to 60 of line 09SN_10LLS-M).

3.4 Hybrid Seismic Data Processing

3.4.1 p-wave *Reflection* Seismic Processing Sequence

A) Data conditioning

A1 Reformatting and quality verification of field data
A2 Recording geometry assignment
A3 Data editing (suppression of bad / dead traces, etc.)
A4 Preliminary analysis of refraction velocities

B Filtering and deconvolution

B1 Analytical muting of refraction arrivals
B2 Amplitude recovery / amplitude equalization in time and frequency domains
B3 Predictive deconvolution parameter tests / application
B4 Determination of band limiting corner frequencies / application
B5 Optional 2-D filtering

C) Velocity analysis and stack

C1 Common Depth Point (CDP) sort
C2 Semblance velocity analysis using supergathers of 3 - 5 CDP's
C3 Optional dip move-out correction
C4 Normal Move-Out (NMO) correction and application of stretch mute
C5 Band-pass filtering
C6 CDP stack
C7 Optional coherency filtering

D) Time-depth conversion

D1 Optional spiking deconvolution
D2 Band-pass filtering
D3 Depth conversion
D4 Final display of seismic depth section with inversed polarity (non-SEG-convention)

3.4.2 The presentation of reflection seismic data

The reflection seismic processing of the p-wave dataset does not give any useful result for lack of reflection events in the nearly homogeneous limestone.

3.4.3 p-wave refraction tomography processing

The seismic p-wave refraction processing steps are analogous to those described in paragraph 3.2. For a detailed method statement and a description of the processing steps please refer to the summary report. The Figs. 3.4a to 3.4c and Tab. 3.4a illustrate the intermediate processing steps and the final result.

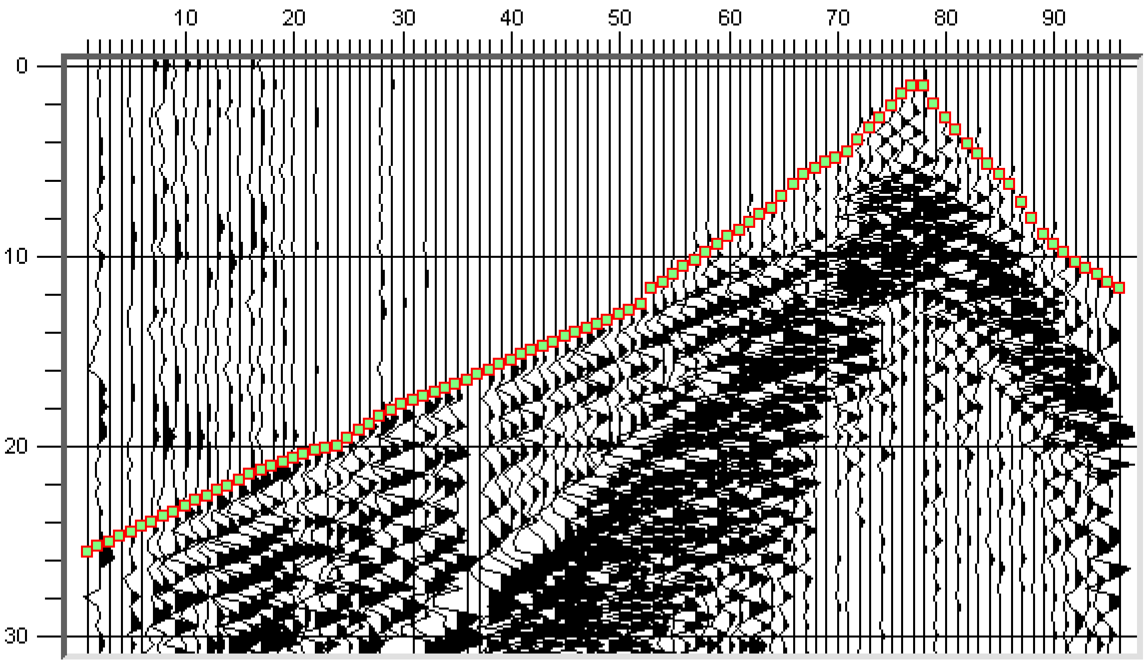

Fig. 3.4a: p-wave records of 09SN_10LLS-P with positive amplitude excursions in black. Colored dots mark the manually picked first break arrival times. Vertical axis: travel time in ms, horizontal axis: station numbers spaced at 1.5 m.

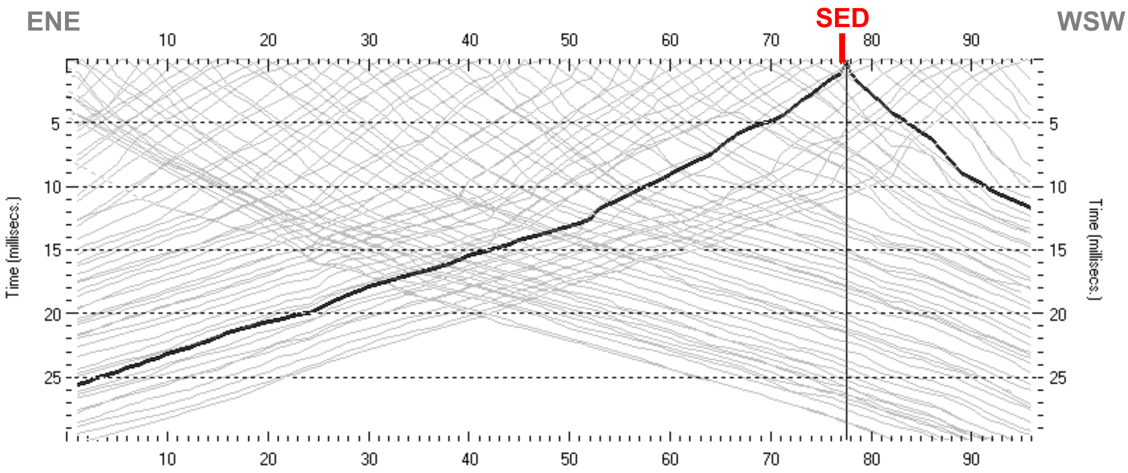

Fig. 3.4b: Travel time curves of p-wave arrival time picks of line 09SN_10LLS-P. Vertical axes: travel time [ms], horizontal axes: station number (= profile meter).

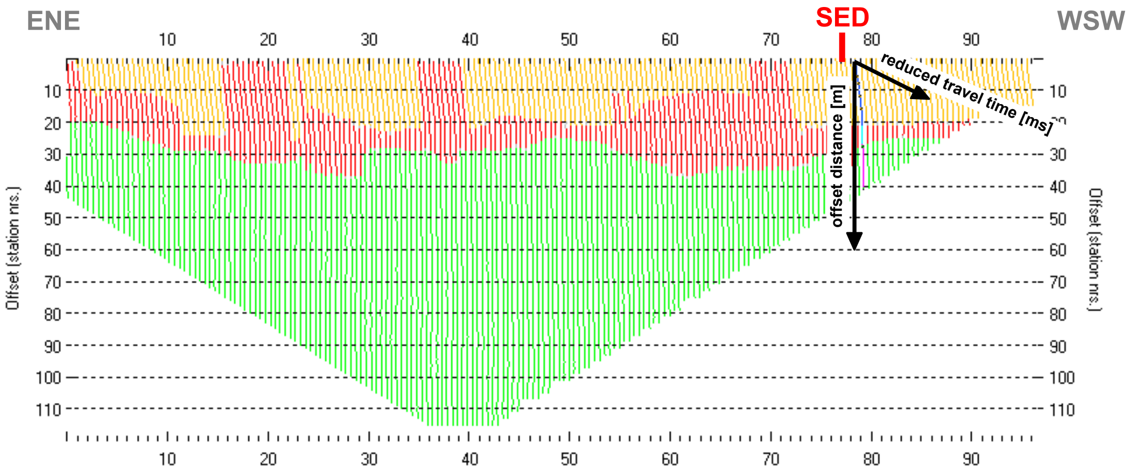

Fig. 3.4c: 3-dimensional distance-travel time diagrams at the mid-points between source points and receiver stations are instrumental when using the analytical CMP derivation of the initial velocity field. The horizontal axes are along the CMP positions and the travel time respectively, the vertical axis denotes the offset distance between source and receiver positions.

Depth [m]	Vp [m/s]
0.2	2877
0.7	2806
1.1	2782
1.8	2792
2.6	2897
3.7	3039
5.1	3237
6.8	3577
9.3	4149
12.3	5107
16.3	5989
21.4	6394
28.0	6283
36.6	6574

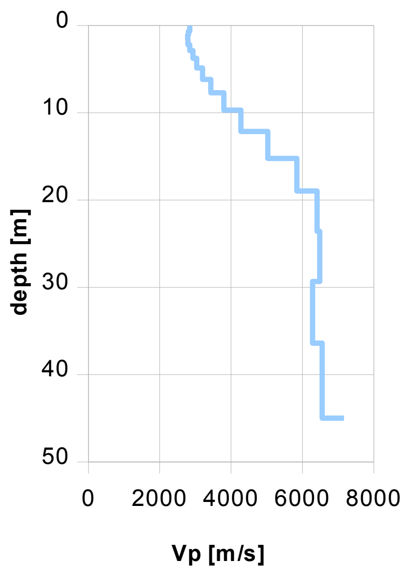

Tab. 3.4a: Initial 1D p-wave velocity model derived from real data of line 09SN_10LLS-P.

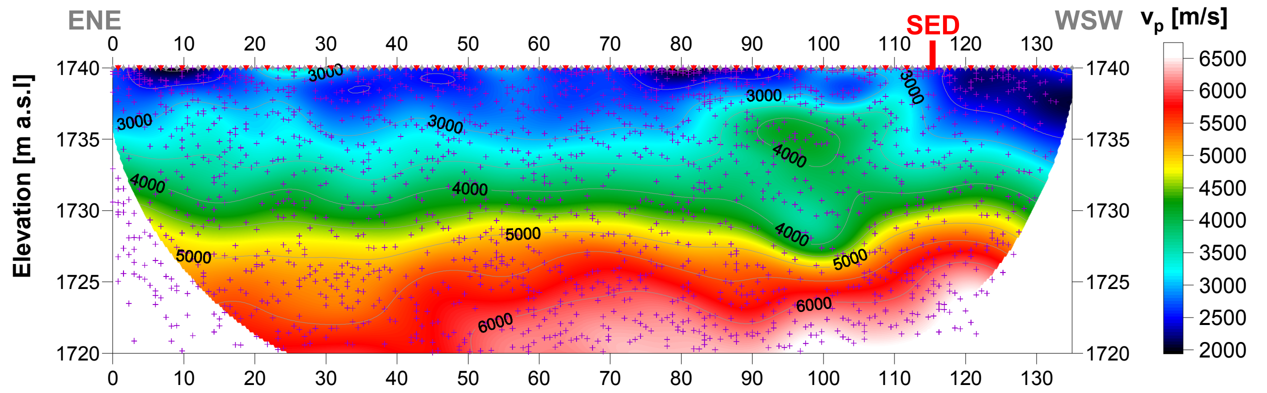

Fig. 3.4d: *Compressional wave velocity field image along the seismic profiles 09SN-10LLS-P . Vertical axis: elevation [m a.s.l]; horizontal axis: profile meter; color scale: v_s [m/s]; vertical exaggeration: 2:1; gray squares: receiver stations; red triangles: shot positions; magenta crosses: positions of determined velocity values.*
The station spacing is 1.5 m, profile meter 0 = line station number 00; profile meter 135 = line station number 90.

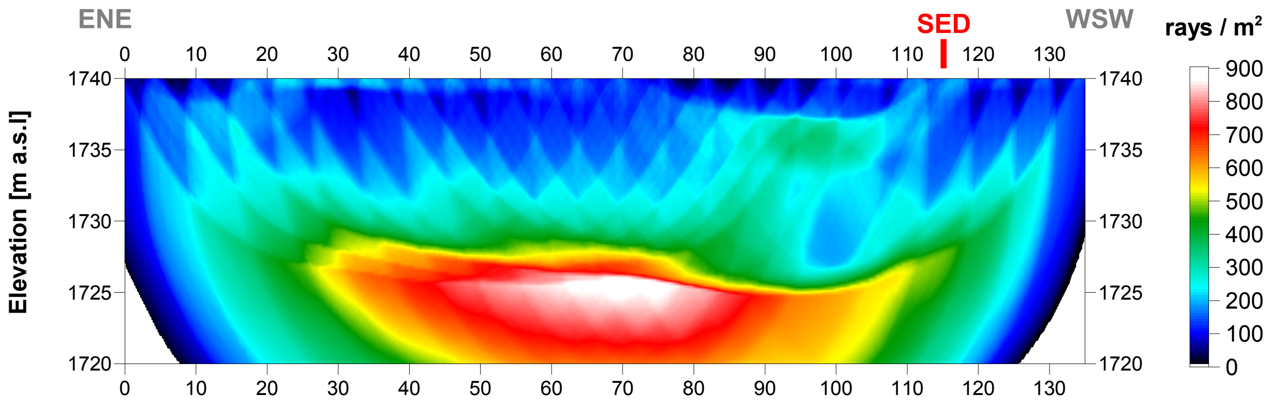

Fig. 3.4e Compressional wave subsurface ray path density along the seismic profiles 09SN_10LLS-P. Red/white colors indicate high velocity contrast between two layers, blue/black colors low coverage areas. Vertical axis: elevation [m a.s.l]; horizontal axis: profile meter; color scale: ray paths per m2; vertical exaggeration: 2:1.

Depth [m]	Vp [m/s]
0.0	2512
1.5	2669
2.9	2875
4.2	3068
5.5	3271
6.8	3540
8.2	3857
9.5	4214
10.8	4622
12.1	5049
13.4	5408
14.8	5659
16.1	5862
17.4	6053
18.7	6181
20.1	6221

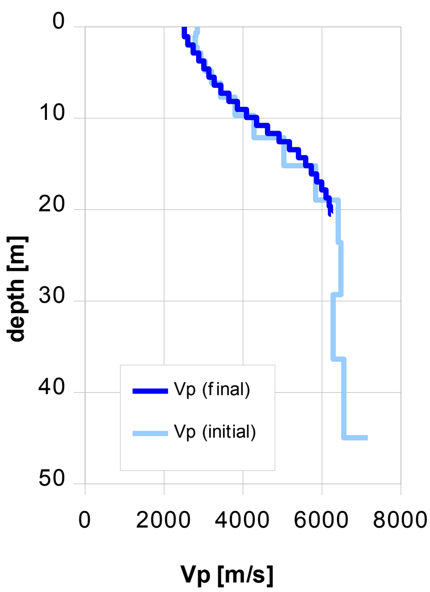

Tab. 3.4b: Final 1D p-wave velocity model derived from real data at positions most similar to the geological setting at SED station between profile station 30 and 60 at line 09SN_10LLS-P. Initial 1D p-wave velocity model values are given in Tab. 3.4a.

4 DISCUSSION OF THE RESULTS

4.1 Summary and Validation of the Results

Compressional and shear wave velocity data from refraction seismic surveys both p-wave and s-wave and also the MASW survey data of profiles 09SN_10LLS-1 are shown in Tab. 4.1 for the uppermost 30 m. The calculated shear wave velocity $v_{s(calc)}$ in Tab. 4.1 is derived by using a theoretical v_p/v_s-ratio of $\sqrt{3}$.

Depth	Vp	Vs	Vs	Vs	Vs1
	refr	refr	calc	MASW65	MASW 135
0.0	2512	2074	1450		
1.0	2598	2517	1500	2968	
2.0	2738	2954	1581	2989	3000
3.0	2875	2987	1660	2978	
4.0	3005	2976	1735	2928	
5.0	3132	2984	1808		2984
6.0	3271	3002	1888	2849	
7.0	3439	2991	1986		
8.0	3644	2931	2104	2762	2822
9.0	3857	2837	2227		
10.0	4088	2692	2360		
11.0	4345	2623	2508	2786	
12.0	4622	2558	2669		2713
13.0	4910	2633	2835		
14.0	5179	2735	2990	3024	
15.0	5408	2845	3122		
16.0	5585	2982	3224		
17.0	5728	3192	3307		2928
18.0	5862	3355	3384	3174	
19.0	5995	3495	3461		
20.0	6104	3553	3524		
21.0	6181	3606	3569		
22.0	6217	3634	3589		
23.0	6231	3664	3598	3313	
24.0		3701			3136
25.0		3745			
26.0		3797			
27.0		3858			
28.0		3919			
29.0		3985			
30.0		4059			

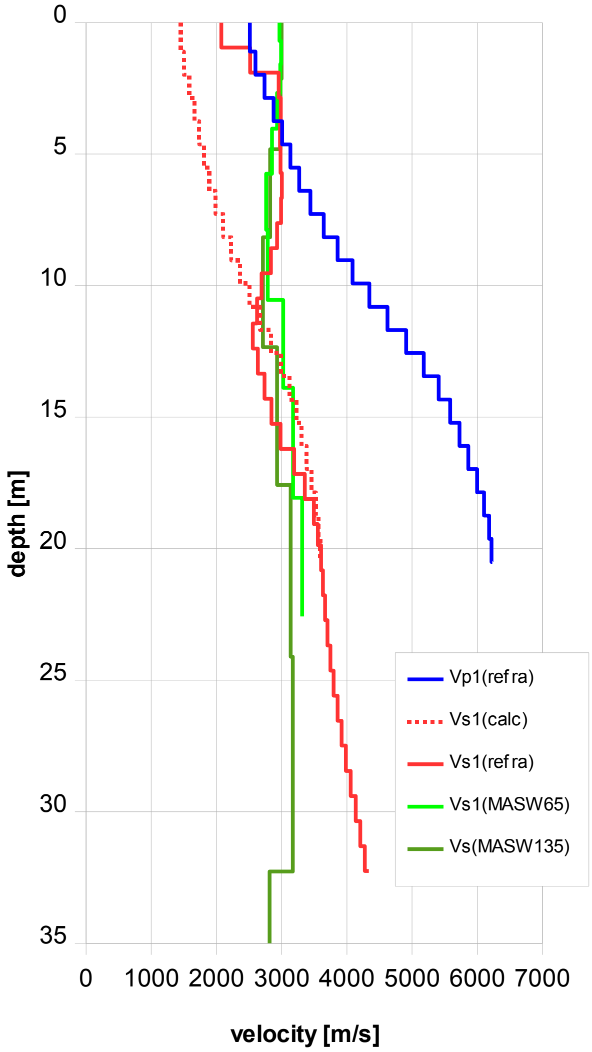

Tab. 4.1: Shear and compressional wave velocity model determined at the SED station LLS.

Fig. 4.1: Graphic display of shear (continuous lines) and compressional (dotted lines) wave velocities determined at the SED station.

The different signal production (= source geometry; see chap. 2.5) leads to different velocity information in the uppermost 3 to 5 meters, especially to too low values in the p-wave velocity image. Because the vertical hammer impacts strike at the concrete basement, the seismic records (Fig. 3.4a) show obviously a two-layer-case with a lower velocity layer covering a high velocity unit. On the other hand, the seismic shear wave records (Fig. 3.2a) seldom show a two-layer-case, mostly a one unit with small varieties in velocity values is found. We explain this observations by the strikes done directly to the limestone.

4.2 Validation of the methods and their results

Due to methodological differences, v_s velocities derived by MASW analysis and by the refraction tomography technique may differ considerably. This is because MASW analysis cannot image small rock/soil inhomogeneities as a dispersion image with an array length of i.e. 65-m only yields one single v_s-value at each depth. On the other hand, refraction diving wave tomography results produce v_s-sections with a high lateral resolution, but fail to provide information at greater depths and in particular with velocity inversions. So the shear wave refraction values are resilient only for the uppermost meters.

4.3 Error Estimates

The error estimates given in Tab. 4.3 below are relevant only in the context of this survey.

Surveying method	Type of result	Error estimate
v_s – refraction tomography	v_s – velocity field image	5 %
MASW only “+” or only “-“ values*	v_s – velocity field image	8 %
MASW (mean of “+” & “-“ values)*	v_s – velocity field image	5 %
v_p – refraction tomography	v_p – velocity field image	5 %**
Reflection seismic surveying	Image of subsurface structures	n.a.

** MASW values in the uppermost 2 - 3 m are prone to an error of about 25 %.*
*** v_p-refraction velocity values in the uppermost 3 - 5 m describe another geological unit (chap. 4.1).*

Tab. 4.3 Error estimates for the methods applied. Note that higher error estimates are to be taken into account with increasing depths.

At the SED station LLS (Linth-Limmern GL), the MASW figures are in the same range as the values obtained from the shear wave diving wave refraction tomography surveys.

5 SUMMARY AND CONCLUSIONS

- In March 2009 a combined seismic s- and p-wave survey was carried out at the SED earthquake monitoring station in a gallery of Linth-Limmern Kraftwerke AG, canton Glaris.
- The shear wave data have been evaluated by conventional diving wave refraction tomography techniques in order to derive the s-wave velocity field along the seismic line. Due to the inherent constraints of the refraction tomography method, the depth of investigation is limited to 10 to 20 m under the prevailing geological conditions.
- The p-wave data have been processed
  - firstly to derive a 2D s-wave velocity field by using the MASW (**M**ultichannel **A**nalysis of **S**urface **W**aves) technique;
  - and secondly, according to the refraction seismic data processing scheme for representing the subsurface p-wave velocity field.
- The shear wave velocity range determined by the MASW method in the uppermost 30 meters spans from values of 2713 m/s to 3313 m/s.
- The scalar values derived by the MASW survey at the SED station (line 09SN_10LLS-1, profile station 45) are the following:

  $v_{s,5}$ = 2987 m/s
  $v_{s,10}$ = 2920 m/s
  $v_{s,15}$ = 2893 m/s
  $v_{s,20}$ = 2943 m/s
  $v_{s,25}$ = 2988 m/s
- The maximum reliable refraction shear wave velocity derived is about 3200 m/s at 17 m depth.
- The maximum reliable p-wave refraction velocity determined is 6200 m/s at 18 m depth.

Schwerzenbach, 29th May 2009

Walter Frei	Lorenz Keller
dipl. Natw. ETH	dipl. Natw. ETH
managing director	project manager